Journal of Manufacturing Systems 84 (2026) 207–222

Contents lists available at ScienceDirect

Journal of Manufacturing Systems

journal homepage: www.elsevier.com/locate/jmansys

Technical paper

A cradle-to-cradle life cycle assessment framework linking machining parameters, tool life and part durability

I. Rodriguez [a,b,*], P.J. Arrazola [a], M. Mori [b], G. Ortiz-de-Zarate [a], A. Madariaga [a], M. Cuesta [a], F. Pušavec [b]

[a] Mondragon Uniberstitatea, Faculty of Engineering, Loramendi 4, Mondragón 20500, Spain
[b] University of Ljubljana, Faculty of Mechanical Engineering, Ljubljana, Slovenia

ARTICLE INFO

Keywords:
Life cycle assessment
Cradle-to-cradle
Sustainable manufacturing
Cryogenic machining
Part durability
Aeronautics
Composite/titanium stacks

ABSTRACT

Machining operations influence sustainability not only through immediate energy and resource use but also through their effects on tool longevity and part durability. Conventional life cycle assessments (LCAs) of machining typically adopt gate-to-gate boundaries, overlooking how machining parameters affect surface integrity, fatigue life, and the frequency of cutting-tool and machined component replacement. This study develops a novel cradle-to-cradle LCA framework that incorporates machining-induced tool wear and part durability into system-level environmental impacts. The approach is demonstrated through a real case study of drilling the CFRP/Ti6Al4V stacks used for the Boeing 787 fuselage, comparing dry drilling with liquid carbon dioxide combined with minimum quantity lubrication (LCO_2+MQL). Experimental tests quantified energy demand, resource consumption, tool life, and hole quality, while part durability was evaluated via fatigue testing and finite element simulations. Results show that the cutting tool production was the dominant contributor to the overall environmental impact. Despite requiring additional auxiliary inputs, LCO_2+MQL drilling reduced overall environmental impacts by 60–70 % relative to dry drilling, due to extended tool life and improved component service life. These findings demonstrate that coolant-assisted machining, when durability and tool-life effects are considered, yields a net environmental benefit. The proposed framework provides a transferable method to expand LCAs beyond gate-to-gate boundaries by integrating the influence of machined part quality on durability and in-service repairs, enabling cradle-to-cradle assessments that better capture the system-level implications of machining decisions.

1. Introduction

Machining is a fundamental manufacturing process for the production of precision parts used in various industries, with a market value of 402 billion dollars in 2024 [1]. There are no direct greenhouse gas emissions as machining is largely electrified. However, there are various environmental impacts related to electricity generation and consumables (cutting tools, coolants/lubricants, etc.) [2].

The concept of circular economy has gained traction among manufacturing companies worldwide as circular material utilization models can increase profitability [3]. According to Kara et al. [4], embracing a circular economy in manufacturing not only reduces the demand for raw materials, but also mitigates environmental impacts, while meeting the social and economic requirements for sustainable production. It is important to increase the longevity of products and materials in circulation by focusing on improved performance, reusability, reparability, remanufacturing and recycling [4]. This applies to machined parts as well as consumables and equipment such as cutting tools, coolants, machine tools, etc.

As illustrated in Fig. 1, there are several potential recovery streams through recycling, repair and reuse to achieve a circular economy in machining. For example, the chips and scraps, coolants and lubricants, tools and other waste streams can be recovered and recycled. As for finished products, repair and reuse cycles would extend the useful life of the component, reducing its environmental impact. In any case, maximizing the recyclability of said parts at the end of their life is critical for increasing the circularity of the system.

The impacts or benefits of these circular strategies are often evaluated using indices and frameworks, with Life Cycle Assessment (LCA) being one of the most widely used tools. LCA, standardized by ISO 14040

* Corresponding author at: Mondragon Uniberstitatea, Faculty of Engineering, Loramendi 4, Mondragón 20500, Spain.
E-mail addresses: irodriguez@mondragon.edu, inigorodriguez2@gmail.com (I. Rodriguez).

https://doi.org/10.1016/j.jmsy.2025.11.021
Received 16 October 2025; Received in revised form 25 November 2025; Accepted 26 November 2025
Available online 15 December 2025

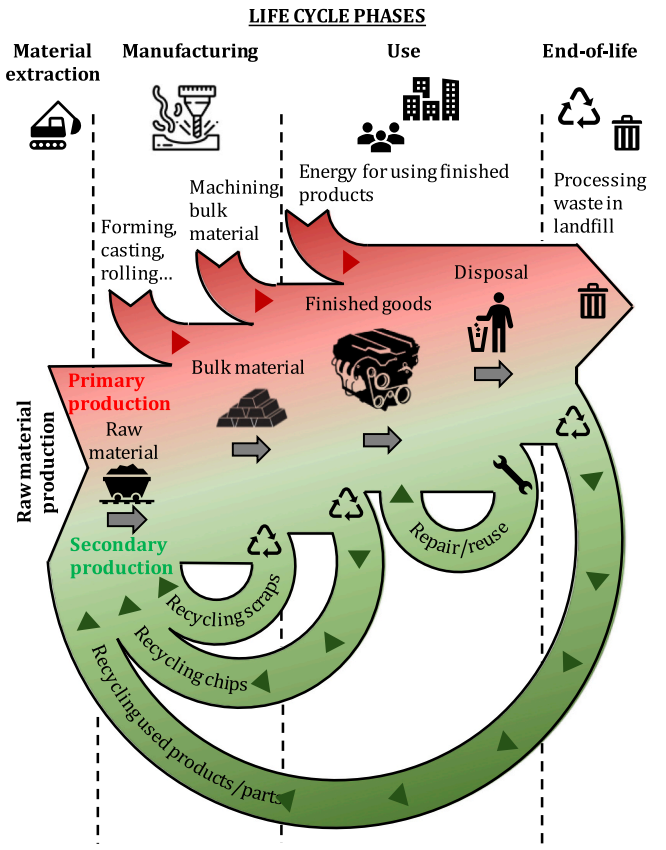

Fig. 1. Consumption sources in machining operations and potential recovery streams across different life cycle phases to achieve circular economy.

and ISO 14044, assesses the environmental impact of products and services along their entire life cycle. The analysis is carried out by defining a functional unit and the boundaries of the system, for then creating an inventory of the relevant inputs and outputs needed to manufacture, use and dispose/recycle the functional unit. Then, the environmental impacts associated to that inventory are assessed. The phases of the life cycle (material extraction, manufacturing, use and end-of-life) of the manufactured product that are considered in the LCA also have a significant impact on the results of the sustainability analysis. For example, a cradle-to-gate analysis only considers the product life cycle from the resource extraction phase to the factory gate (before the finished part is transported to the consumer), as defined in [5]. A cradle-to-grave analysis also takes into account the impacts generated during the use and disposal of such product, and if the regenerative flows (recycling, repair, remanufacturing) are included in the analysis, it would become a cradle-to-cradle analysis.

Furthermore, the different input material and energy flows involved in a machine-tool system interact and influence each other across the different life cycle phases. An example of this is given in Fig. 2. As can be seen, different input flows (coolant, tool material and coating, machining parameters, clamping fixtures, etc.) not only affect process sustainability through direct use of energy and resources to generate these inputs, but also influence machining performance. This, in turn, affects sustainability through cutting tool service life and machine-tool energy consumption. Salem et al. [6] proposed an approach to integrate part quality in the sustainable machining metrics, however, without considering part durability and thus, not taking into account the impact of part service life on the overall resource and energy consumption, along the life cycle.

For example, longer tool life through the use of coolants or coated tools reduces the environmental impact associated with the manufacture of cutting tools (embodied energy of the tools), and the energy consumption associated with tool changes [7–9]. On the downside, employing coolants or coatings creates additional resource consumption [10]. Therefore, to achieve a sustainable machining process, the energy and material savings in the machine-tool system must outdo the energy and resource consumption required for the production, use and disposal of such coatings and coolants. Other factors such as machining parameters can affect the energy consumption and tool life, and the clamping can affect the appearance of chatter leading to premature failure of the tool [11].

Table 1 summarizes the main LCA and energy consumption studies on machining operations. Most of the studies investigated the influence of the coolant on the environmental impacts caused by the machining process. This is because the coolant is one of the factors that has the most direct impact on the resource and energy consumption of the machine-tool (cutting fluid consumption, energy required for the pumps, etc.) [12]. However, not all of them account for the environmental impact derived from tool wear, which can be a more relevant factor than the electric energy consumption of the machine due to the energy requirements to produce tool materials [13]. Regarding the boundaries of the LCA systems in Table 1, most works employ gate-to-gate or cradle-to-gate scopes, therefore confining the analysis to the resource consumptions occurring during the machining operation. Moreover, the impact created during the use phase of the fabricated component is not considered by any of the studies, and very few take into account the resources needed or recovered at the end-of-life phase. Gate-to-gate studies exclude upstream flows (e.g., tool and material production) and downstream flows (e.g., product use, repairs and replacement). Having a restricted scope can misrepresent sustainability trade-offs because durability-related effects which are influenced by the machining process are invisible outside the factory gate. This was also highlighted by Kokare et al. [14] who claimed that extending the scope of LCA in additive manufacturing was a key future step to prevent manufacturers from getting misleading conclusions from studies covering part of the life cycle. Favi et al. [15] also emphasize the relevance of increasing the durability of components being one of the key aspects to sustainable manufacturing.

Including all life cycle stages when conducting an LCA of a manufactured part is a complicated process due to the input and output flows interacting across the different life cycle phases [2], as shown in Fig. 2. However, this is a crucial aspect to achieve a more accurate estimation of the environmental impact created by the process, especially knowing that machining is usually one of the last operations in the production chain. This means, that the machining operations will determine the surface integrity of the components, which affects their in-service performance and durability (i.e. fatigue and corrosion resistance) [32,33], and consequently the environmental impact they create during the use phase. Despite this influence of part durability on sustainability being known, to the best of the authors' knowledge, it has never been quantitatively integrated into LCA frameworks. Interestingly, considering the durability of machined components could justify using additional input streams, if they help reduce the impact caused by the need of fabricating new ones [10].

In this work, the influence of surface integrity on fatigue life is characterized experimentally, and part durability is modelled to estimate product repair frequency, and its effect on sustainability. This allows the development of a novel cradle-to-cradle LCA framework for

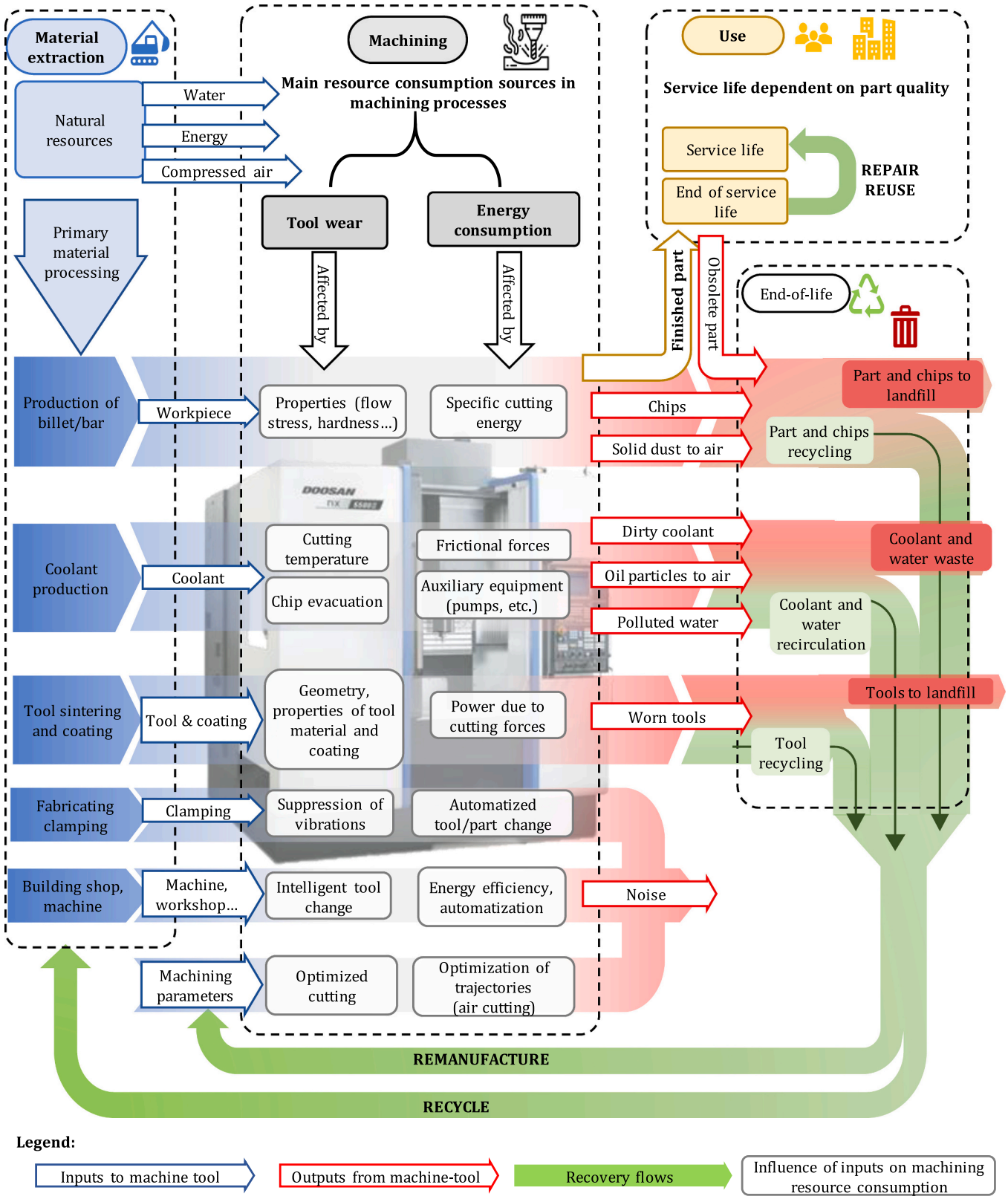

Fig. 2. Influence of machining inputs on the environmental performance of the process, the resulting output flows generated during part production, and the potential recovery flows contributing to circular economy strategies. The diagram illustrates how different machining inputs affect process performance and the associated environmental outflows, across all life cycle phases.

Table 1
Summary of most relevant LCA and energy consumption studies in manufacturing, and life cycle phases considered. E: resource extraction; M: manufacturing; U: use; EoL: end-of-life (Tool wear considered in machining: ◐ no / ● yes).

Reference	Process	Analysis	Varied input	Functional unit	LCA phases considered			
					E	M	U	EoL
[16]	Turning	LCA	Coolant	1year production	●	◐		
[17]	Turning	LCA	CoolantMachining parameters,	Not defined	●	◐		
[18]	Friction drilling	LCA	Coolant	400 holes	●	◐		
[19]	Turning	Energy	CoolantWorkpiece material,	One turning pass	●	●		
[20]	Grinding	LCA	Wheel typeMachining parameters,	3 cm^3 of machining	●	●		
[21]	Turning	Energy	Coolant	5 cm^3 of machining	●	●		●
[22]	Drilling	LCA	Coolant	One hole	●	◐		●
[23]	Turning	Energy	Coolant	1cm^3 of machining	●	●		
[24]	Milling	Energy	CoolantMachining parameters,	1cm^3 of machining	●	●		
[25]	Milling	CO_2 emissions	CoolantTool geometry,	1cm^3 of machining	●	◐		
[26]	Drilling	LCA	Coolant	One drilled hole		●		
[27]	Turning	LCA	Coolant	1 min of cutting	●	◐		
[28]	Turning	CO_2 emissions	Coolant	10 cm^3 of machining	●	◐		
[29]	Turning	Energy	Coolant	140 mm machined	●	◐		
[30]	Turning	Energy	Coolant	10 min of machining		◐		
[31]	Turning	Energy	Machining parameters	Different machining features		◐		

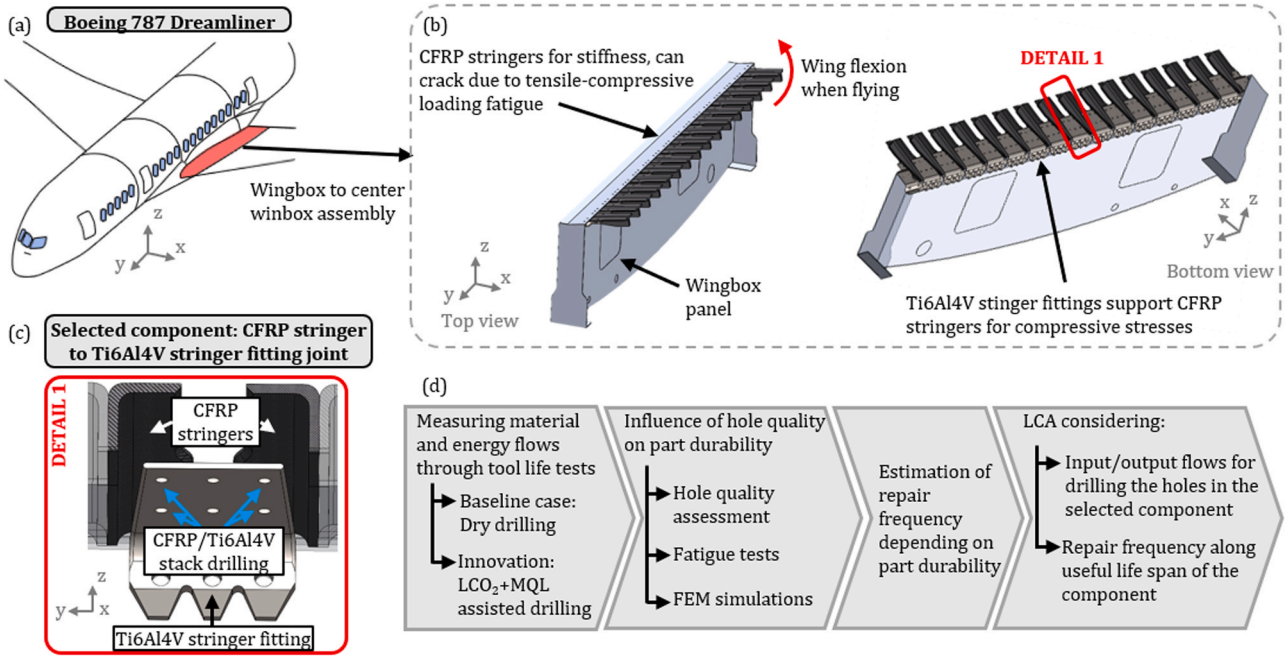

Fig. 3. (a) Location of CFRP/Ti6Al4V stack components in a Boeing 787 Dreamliner; (b) Detail of wingbox assembly; (c) Drilling operation selected for the case study, (d) Workflow carried out in this research.

machining that couples machine-level resource use with measured tool wear and part durability. The framework is applied to a CFRP/Ti6Al4V stack drilling case study for the Boeing 787 fuselage, comparing dry drilling with liquid carbon dioxide plus minimum quantity lubrication (LCO_2+MQL). Resource and energy demand were monitored, while fatigue tests and FEM simulations quantified part durability. These data were compiled into a life cycle inventory (LCI) to generate environmental indicators for the tested drilling strategies and to assess their system-level impacts.

The novel contributions of this work are threefold: (i) a surface integrity-aware cradle-to-cradle LCA is developed linking machining parameters to tool life and part durability; (ii) it demonstrates that additional resources can be environmentally beneficial when they improve machined component performance; and (iii) it proposes a generalizable workflow for extending manufacturing LCAs wherever surface integrity governs service life.

2. Cradle-to-cradle Lca modelling for machining

2.1. Selected case study, materials and experimental methodology definition

The selected case study was based on a component that is usually machined in dry conditions, namely the CFRP/Ti6Al4V stacks found in aviation. Composite/metal stacks such as CFRP/Ti6Al4V are widely used in aeronautics as they combine the mechanical properties of both materials [34]. Although this hybrid stack is a difficult-to-cut material due to the challenges it presents in terms of poor tool life and bad machined surface quality [35], conventional coolants and lubricants cannot be employed to alleviate these problems. This is due to the potential moisture problems that the emulsion coolants can create on the composite material, degrading its mechanical properties [36]. Therefore, this material is usually drilled in dry. However, alternatives are being explored to provide cooling and lubrication in the cutting zone without flooding it excessively, such as sub-zero cooling and lubrication

Table 2
Material properties of the Ti6Al4V titanium alloy at room temperature, provided by the supplier.

Yield strength [MPa]	921
Tensile strength, Ultimate [MPa]	1048
Young's modulus [GPa]	105
Poisson's coefficient [-]	0.31
Elongation [%]	12.5

Table 3
Material properties of CFRP composite reinforcement fibers and epoxy matrix at room temperature, provided by the supplier.

Reinforcement fibers	Sigratex CW205 TW282
Areal weight [g/m^2]	205
Tensile strength [MPa]	2400
Young's modulus [GPa]	300
Elongation [%]	1.7
Density [g/cm^3]	1.8
Fiber volume fraction [-]	0.5
Epoxy matrix	Hexcel Hexflow RTM 6–2
Tensile strength [MPa]	75
Tensile modulus [GPa]	2.9
Elongation [%]	3.4
Density [g/cm^3]	1.14

with LCO_2+MQL [34].

The case study was based on the fabrication and repair of components of a Boeing 787 Dreamliner, as they have reported CFRP/Ti6Al4V structures in the connection between the aircraft fuselage and wings, also known as the wingbox to center wingbox assembly (Fig. 3a). In this critical joint, the CFRP stringers, which provide stiffness to the wing, are supported by Ti6Al4V stringer fittings (Fig. 3b). This solution, first introduced by Boeing to avoid cracks in CFRP stringers when the wings flex [37], involves a series of bolted holes in the CFRP/Ti6Al4V stacks (Fig. 3c), which are normally drilled in a single operation to reduce positioning errors [34].

The procedure for evaluating the environmental impact of the selected component when machined under different cooling/lubrication conditions is summarized in Fig. 3d:

- First drilling tool life tests were carried out on CFRP/Ti6Al4V plates (mechanical properties given in Table 2 and Table 3) to characterize the input and output flows in each machining condition. Namely, the consumption of resources like cutting tools, coolant or workpiece material, and the energy consumed by the machine-tool. Outflows directly created by the machining process like the airborne particle emissions were also experimentally measured.
- After the machining experiments, the hole quality was analyzed, and specimens were extracted from the drilled CFRP/Ti6Al4V stacks to perform open hole fatigue tests. The experimentally obtained fatigue strength data was then introduced in a FEM study of the stringer to stringer fitting modelled following the US9731,808 B2 and EP 2 842 030 A patents. This allowed us to qualitatively compare the fatigue strength of the component drilled in dry and with LCO_2+MQL. Knowing the durability of the component and the repair procedure [38], the resources and energy needed to manufacture and repair the CFRP stringer to Ti6Al4V stringer fitting assembly along the entire expected life of the Boeing 787 Dreamliner could be estimated.
- Finally, a LCA was carried out considering the input and output flows required to perform the drilling and repairs during the expected life of the aircraft.

2.2. Experimental plan

The LCO_2+MQL was supplied through a single channel at a LCO_2 mass flow rate of q_{LCO2} = 100 g/min and a MQL flow rate of q_{MQL} = 40 mL/h following [39], for dry drilling no coolant was employed. (Fig. 4a). The fixed experimental inputs of the drilling tests included the machining parameters (V_c = 75 m/min, f_n = 0.1 mm/rev), the drill bit

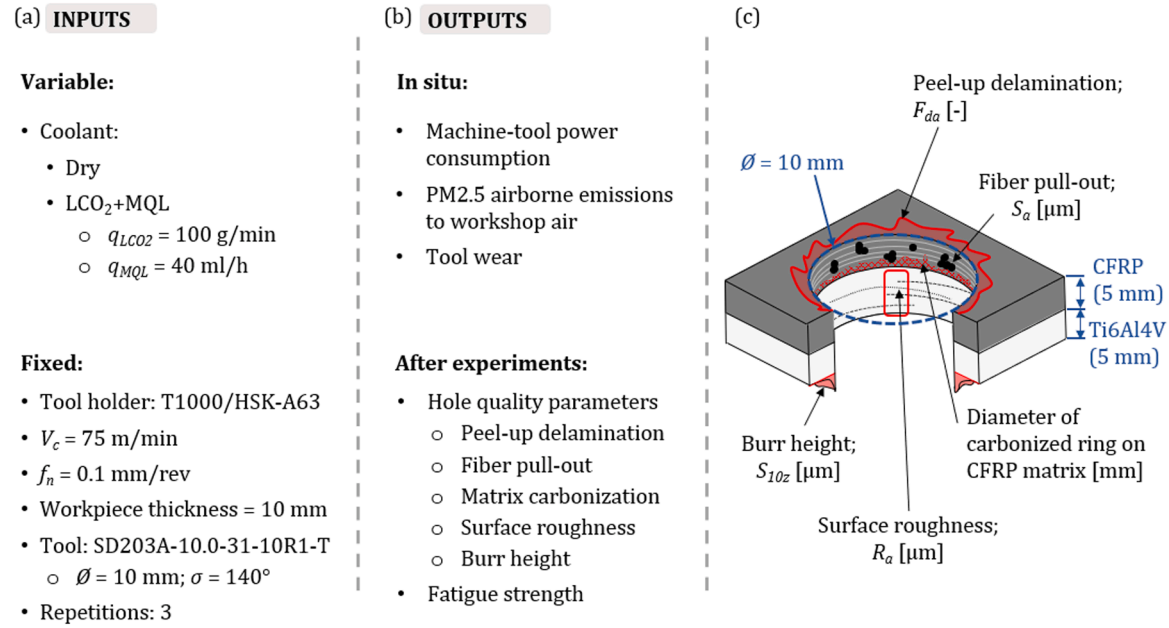

Fig. 4. (a) Fixed and variable input parameters; (b) Output parameters measured in-situ during the tool life drilling tests and after the drilling operation; (c) Analyzed hole quality parameters.

geometry (SD203A-10.0–31–10R1-T), tool material and coating (uncoated carbide), tool holder (Thermogrip T1000/HSK-A63 shrink fit) and the workpiece thickness. Both CFRP and Ti6Al4V plates were 5 mm thick, forming a 10 mm stack, as seen in Fig. 4c. The tool life tests were interrupted every 15 holes to measure the flank wear of the tool according to the ISO 3685 using a Leica DMS 1000 digital microscope with a × 30 magnification. Three repetitions were carried out per condition to determine the uncertainty of the tests. The input streams for the LCA measured in-situ during the tool life tests included the power consumption of the machine-tool, measured via internal signals, and the tool wear (Fig. 4b). Regarding the outputs generated during the machining process, PM2.5 airborne emissions were sampled every 1 s using a DustTrak DRX 8533EP aerosol monitor, as this indicator is an impact category in LCA methodologies.

After the tool life tests were completed, a range of hole quality parameters were evaluated, namely peel-up delamination, fiber pull-out and matrix carbonization at the CFRP phase of the stack, and surface roughness and burr height for the Ti6Al4V phase (Fig. 4c). The peel-up delamination was observed using the Leica DMS 1000 digital microscope (×30 magnification), and evaluated following the advanced delamination factor (F_{da}) proposed by [40]. For the fiber pull-out, the drilled surfaces were characterized using an Alicona IF G4 optical 3D microscope (×10 magnification), using the areal surface roughness (S_a) parameter to define the level of fiber pull-out, as described in [41]. The matrix carbonization at the interface was observed using the Leica DMS 1000 microscope, and evaluated by measuring the diameter of the discolored ring of epoxy [42]. Regarding the Ti6Al4V phase, the machined hole surface and exit burrs were scanned in the Alicona IF G4 optical microscope. The average surface roughness (R_a) was measured to evaluate the quality of the surface finish, and the average ten-point height (S_{10z}) to characterize the burr height. After characterizing the hole quality, the fatigue strength of the drilled holes was analyzed in an MTS 810 material fatigue testing system, following the open-hole fatigue testing procedure (EN 6072).

2.3. Experimental setup

The tests were carried out in a Doosan NX6500 II CNC machining center (Fig. 5a) equipped with a through the spindle delivery for LCO_2+MQL cooling and lubrication. The flow rate control of the coolant and lubricant media was achieved with the Arclub One system. A backup plate was employed for indexing the CFRP/Ti6Al4V stacks and drilling the matrix of holes for the tool life experiments. PM2.5 emissions were measured using a DustTrak DRX 8533EP aerosol monitoring device, following the procedure described in [43].

The open-hole fatigue tests were carried out using an MTS 810 material testing system (Fig. 5b). A tensile/compression sinusoidal loading cycle was applied ($R = -1$) in order to simulate the alternating loads to which the CFRP stringer to Ti6Al4V stinger fitting joint of an aircraft is subjected (Fig. 5d). In this type of fatigue test a cyclic load is applied to the specimen, varying from a defined tensile load to a compressive one. Different load levels were tested at a constant frequency of 5 Hz, to obtain the curves that define the number of cycles to failure (S-N curves). It should be noted that CFRP and Ti6Al4V specimens were tested separately. The design of the fatigue specimens is described in detail in Section 2.4.

The tested loading conditions were determined by carrying out a preliminary sensitivity analysis. Starting at 50 % of the yield strength of each material, the fatigue stress amplitude was increased or decreased in 15 MPa increments depending on the fracture of the specimen until the optimum conditions for fatigue testing were reached. These preliminary tests showed that at stresses below 35 % of the yield strength of the material, the fatigue life was infinite (over 1000,000 cycles) while applying a stress greater than 80 % of the yield strength would fracture the specimen in less than 100 cycles.

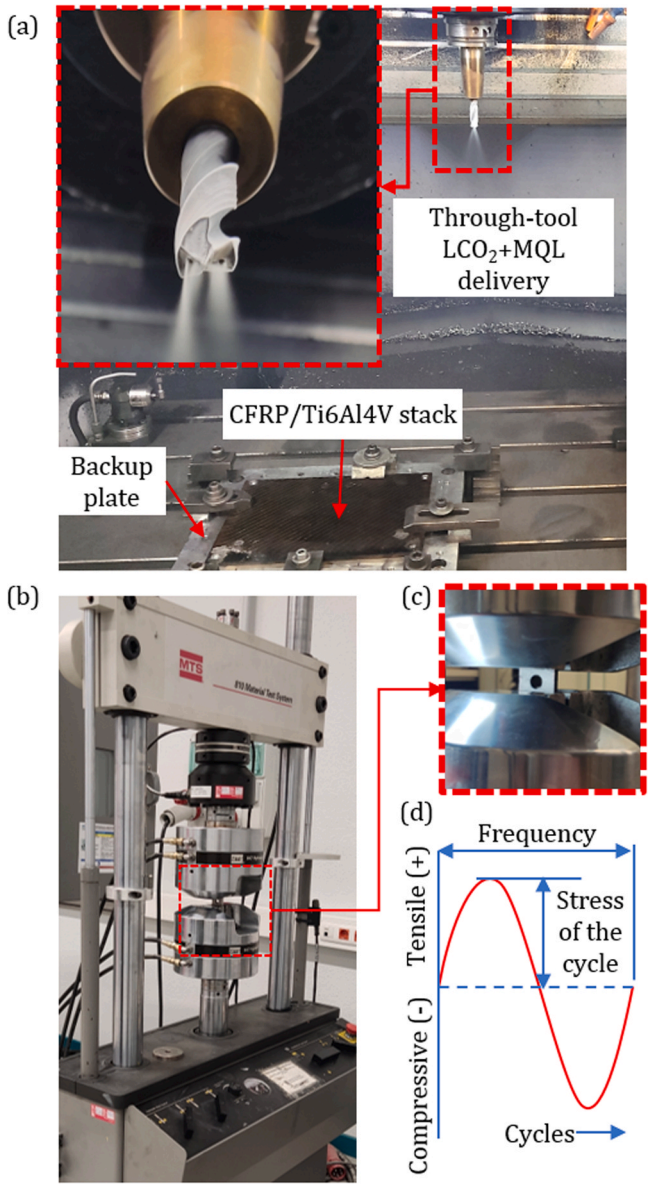

Fig. 5. (a) Machining setup for tool life tests; (b) Fatigue testing setup; (c) Detail of clamped specimen in the fatigue testing machine; (d) Applied loading cycle for the fatigue tests.

2.4. Fatigue specimen design

The distance between holes in the matrix drilled in the CFRP/Ti6Al4V stacks did not allow to extract open-hole fatigue specimens according to the geometry specified in the EN 6072 (Fig. 6a). Thus, an adapted fatigue test geometry was proposed for this study (Fig. 6b). The proposed geometry had a shorter length than the one specified in the EN 6072; however, the rest of the dimensions were maintained. Moreover, when clamping the fatigue specimens produced in this study, the clamps

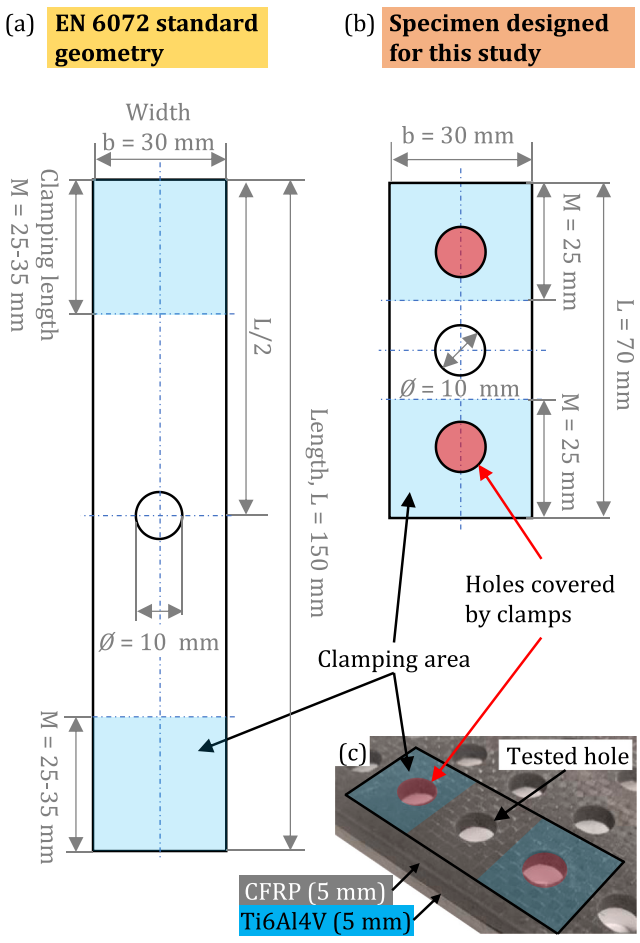

Fig. 6. Open-hole fatigue testing specimen geometry: (a) Defined by the EN 6072 standard; (b) Proposed for this study; (c) Specimen geometry extracted from the drilled plates.

covered drilled holes (Fig. 5c). This was due to the limitations of having a matrix of holes drilled with a separation of 20 mm in the CFRP/Ti6Al4V stacks. The proposed geometry was extracted from the drilled plates, as shown in Fig. 6c, and an experimental and FEM validation of the specimens was carried out to demonstrate that the stress concentration around the central hole and clamping zones was similar to that achieved with the specimen geometry defined in the EN 6072 standard.

3. Results and discussion of the case study

The presentation of experimental results is structured as described in the methodology section. First, the flank wear progression achieved with each cooling/lubrication condition is presented. Then, the hole quality parameters described in Fig. 4c are evaluated, and the fatigue strength results achieved by the CFRP and Ti6Al4V specimens extracted from the stacks drilled in dry and with LCO_2+MQL are shown. Last, the LCA results are given, considering the measured inputs and outputs.

3.1. CFRP/Ti6Al4V stack drilling

The tool life and hole quality results were extracted as the tool wear progressed. The evolution of tool wear and its effect on different hole quality parameters of the CFRP and Ti6Al4V phases of the stack are discussed in the following subsections.

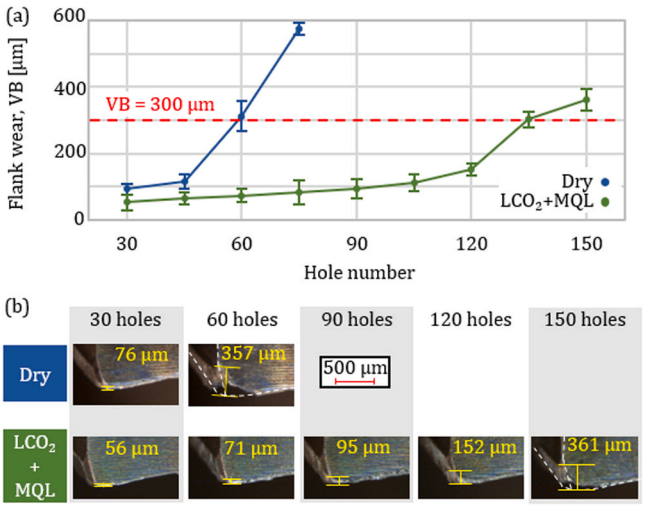

Fig. 7. (a) Tool wear evolution for dry drilling and LCO_2+MQL assisted drilling cases; (b) Microscope images of flank wear.

3.1.1. Tool life

The flank wear (VB) progression for CFRP/Ti6Al4V stack drilling in dry conditions and with the assistance of LCO_2+MQL cooling and lubrication is shown in Fig. 7a. As can be seen, the tools reach the wear limit after approximately 60 holes when dry drilling, whereas 135 holes can be drilled when using through the tool LCO_2+MQL, resulting in a 225 % increase in tool life. Fig. 7 shows that a steady wear development occurs before it increases exponentially, leading to failure. It can also be seen that LCO_2+MQL prevents excessive wear in the corner of the drill bit, resulting in a longer tool life (Fig. 7b).

3.1.2. Hole quality

Regarding the hole quality of the CFRP phase of the stacks, using LCO_2+MQL cooling/lubrication increased the peel-up delamination at the entry plane (Fig. 8a, d and e). This could be due to an increase in the thrust force caused by the cold temperature of the LCO_2 [44]. On the other hand, the temperature reduction by the LCO_2 decreased the matrix carbonization at the exit plane of the CFRP even at high wear levels (Fig. 8c). The carbonization damage is created by the heat that builds up when drilling the Ti6Al4V. The titanium plate and chips can reach temperatures up to 500 °C when drilled in dry, degrading the epoxy matrix [45]. The lower cutting temperatures together with a better chip evacuation when delivering LCO_2+MQL through the tool, minimizes the damage created by the Ti6Al4V chips on the already machined CFRP hole surfaces (Fig. 8b, d and e). The voids in the machined CFRP surface, along with the delamination, can act as crack initiators for CFRP components, thus influencing the fatigue strength of the component.

Fig. 9 sets out the evolution of the surface roughness and burr height of the Ti6Al4V phase of the stack with tool wear. A comparable surface roughness was achieved for dry and LCO_2+MQL assisted drilling when the tool was fresh (Fig. 9a). However, as tool wear progressed, smoother surfaces were achieved with LCO_2+MQL compared to dry drilling, even achieving a better surface roughness at the end of the tool life than that of dry drilling. The 3D surface profiles shown in Fig. 9c and d show that lower burrs are achieved when drilling with LCO_2+MQL assistance than under dry conditions. This could be due to a reduction in the cutting temperature, and thus in the plastic deformation of the Ti6Al4V at the exit plane. The burr height achieved by LCO_2+MQL assisted drilling was homogeneous during the life of the tool. For dry drilling however, a rapid increase was observed as the tool worn out (Fig. 9b).

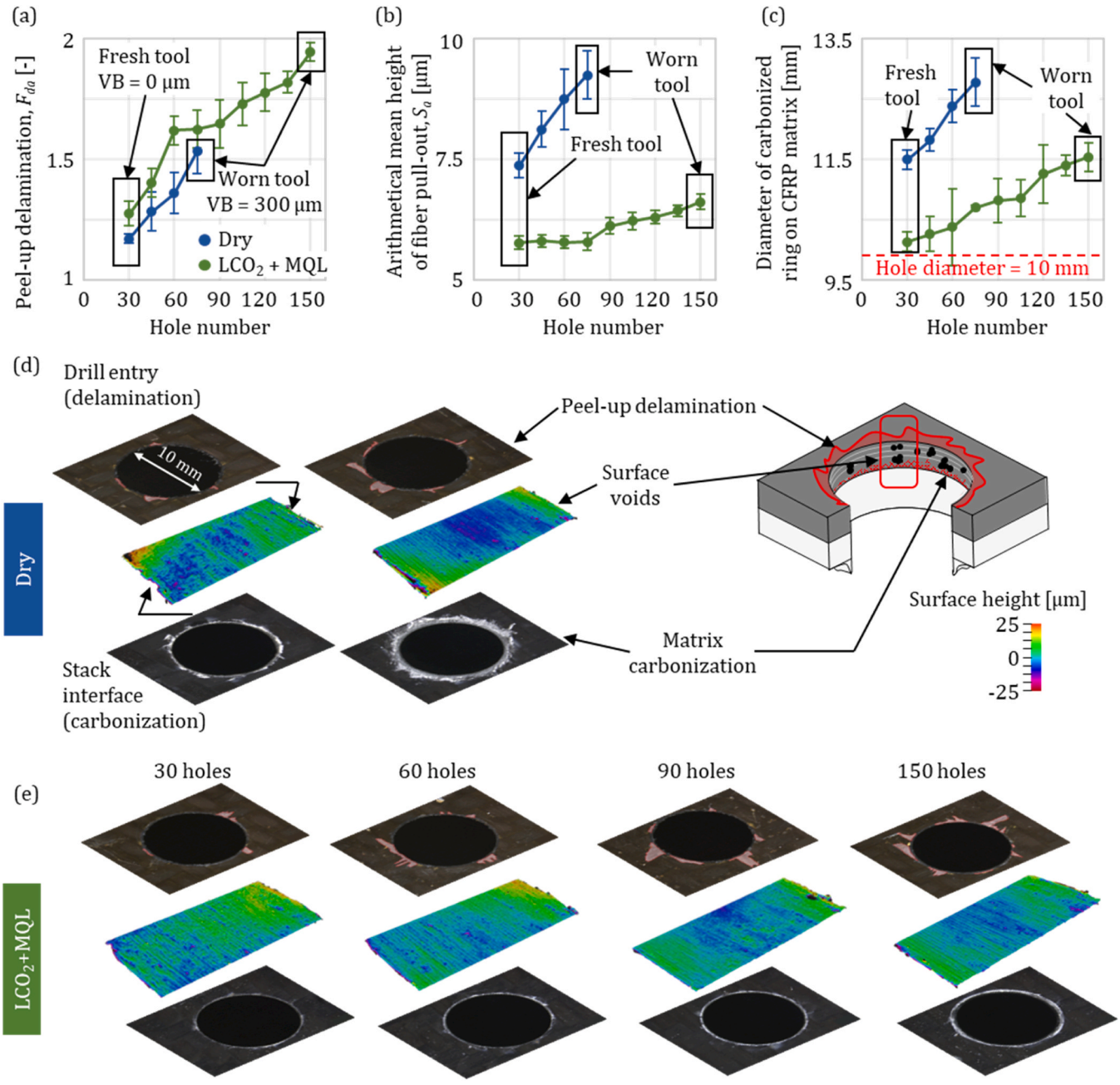

Fig. 8. Hole quality assessment of the CFRP phase of the stack: (a) Peel-up delamination; (b) Arithmetical mean height, S_a; (c) Diameter of discolored ring; (d) Hole quality evolution in dry drilling; (e) Hole quality evolution with LCO_2+MQL.

3.2. Fatigue tests

3.2.1. Specimen geometry validation

The proposed specimen geometry for the fatigue tests based on the EN 6072 standard, was validated through FEM simulations. A uniaxial tensile test was simulated using SolidWorks Simulation software with both specimen geometries. The clamps of the MTS fatigue testing machine were modelled as follows: the lower pair of clamps were fixed, while a roller boundary condition restricting movement in x and z directions was applied to the top pair (Fig. 10a). High order quadratic elements with a size of 1 ± 0.1 mm were employed to correctly calculate the stress distribution around the hole. A nominal stress of 300 MPa (30 kN/100 mm^2) was applied to a specimen with Ti6Al4V material properties (see Table 2), and the maximum stress concentration that occurred at the central hole of the specimen was measured.

As Fig. 10b shows, the stress profiles along the central holes come into good agreement for both fatigue specimen geometries, and the maximum stress concentration occurs at the inner surfaces of the drilled hole. Therefore, it is expected the crack to initiate from that zone. The simulations were validated experimentally by measuring the displacement (δ_y) in experimental uniaxial tensile tests using the MTS 810 machine. Fig. 10c shows the stress – displacement experimental curve. The predicted displacement for a 30 kN load agrees well with the one measured experimentally. Since the stress field around the central hole of the designed specimen was similar to the stress distribution achieved in the specimen defined by the EN 6072, the proposed geometry was validated for the fatigue tests, and the direct comparison of S-N curves between standard and custom geometries is justified.

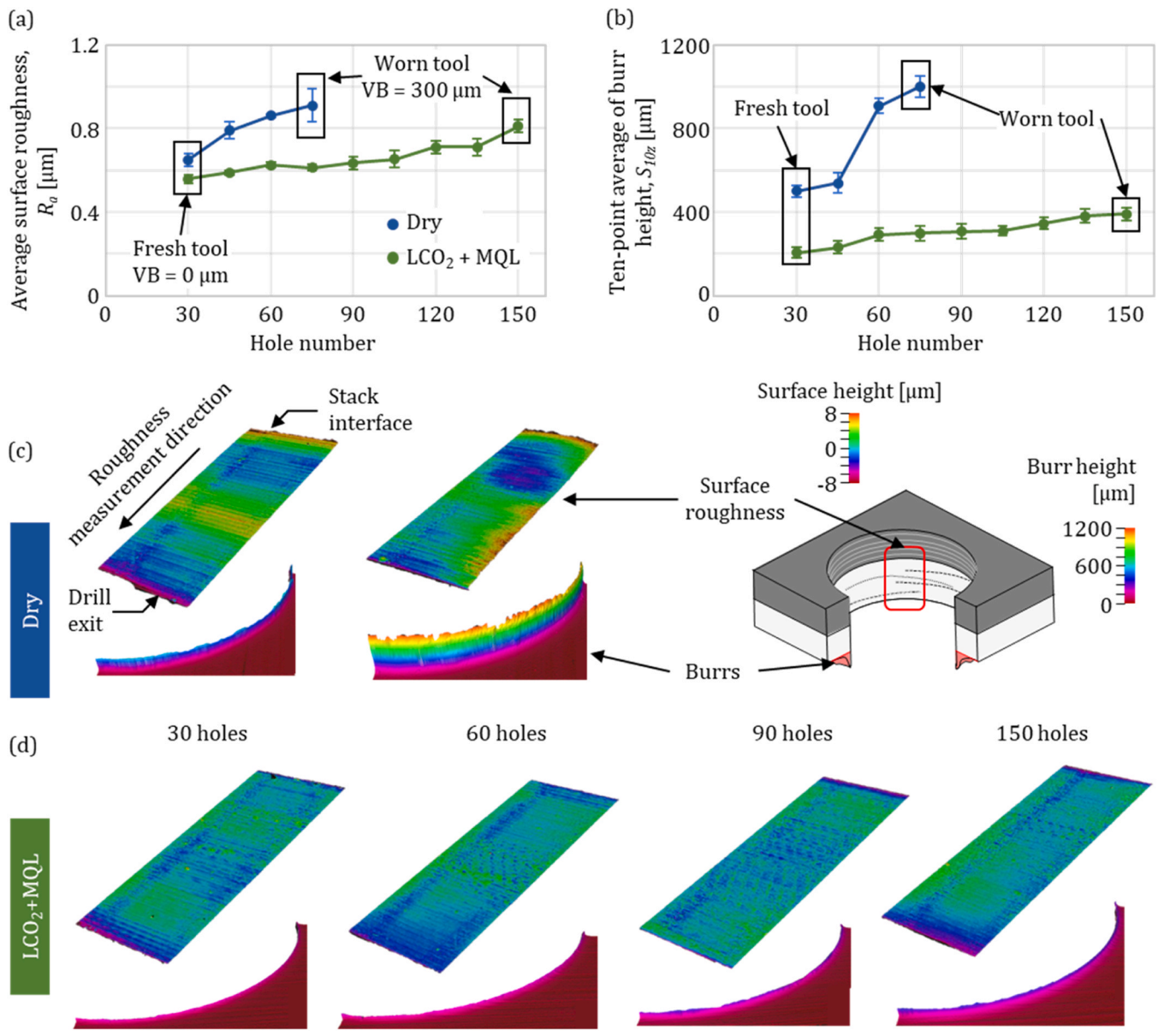

Fig. 9. Hole quality assessment of the Ti6Al4V phase of the stack: Average surface roughness, R_a; (b) Then point average of burr height, S_{10z}; (c) Hole quality evolution in dry drilling; (d) Hole quality evolution with LCO_2+MQL.

3.2.2. *Fatigue tests*

The S-N curves for CFRP and Ti6Al4V plates drilled in the stack are given in Fig. 11. For the CFRP specimens (Fig. 11a) no differences in fatigue strength are seen despite the better hole quality with LCO_2+MQL assistance (reduced matrix carbonization and voids in the machined surface). The specimens broke after a small number of cycles when the stress exceeded 270 MPa, while they lasted more than 1000,000 cycles for loads below 250 MPa. This behavior suggests a material defect-dominated crack initiation. When inherent laminate imperfections (e.g., cut fibers, voids, waviness) govern crack nucleation, machining induced defects become secondary, and an improved hole quality does not necessarily increase fatigue life. Sudarsono et al. [46] similarly reported fiber cuts generated during machining, regardless of the specific machining parameters, govern the open-hole fatigue behavior of CFRP and outweigh other drilling-induced defects at comparable stress levels. Haeger et al. [47] likewise found no direct correlation between machining induced delamination and fatigue crack initiation in flexural tests, while Alam et al. [48] highlighted that laminate manufacturing defects are the primary drivers of CFRP fatigue variability. Overall, these findings suggest that in CFRP, intrinsic laminate defects can dominate fatigue performance over machining-induced defects.

By contrast, the results for Ti6Al4V (Fig. 11b), consistent trends in fatigue strength were achieved for the specimens drilled in dry conditions and with LCO_2+MQL assistance. It can be seen that parts with a higher fatigue strength were produced when drilling with LCO_2+MQL. The fracture surfaces in Fig. 11c, observed under the Scanning Electron Microscope (SEM), show that the crack propagation developed outwards from the drilled hole, as expected from the stress distribution obtained in the FEM simulations shown in Fig. 10. The light and shiny surface close to the hole cross section shows brittle fracture due to crack propagation, and the following dark and matt surfaces show ductile fracture. As seen in areas 1 and 1.A in Fig. 11c, the fatigue crack nucleated from the burr area of the drilled hole, and propagated along the cross section of the sample. The ductile fracture area revealed dimpled surfaces, resulting from the plastic deformation as the specimen failed (area 2 in Fig. 11c). Tool wear affected more the behavior of the samples produced under dry conditions (Fig. 11b), this was probably due to the rapid increase in hole quality defects for the holes drilled in dry with worn tools (Fig. 9a and b).

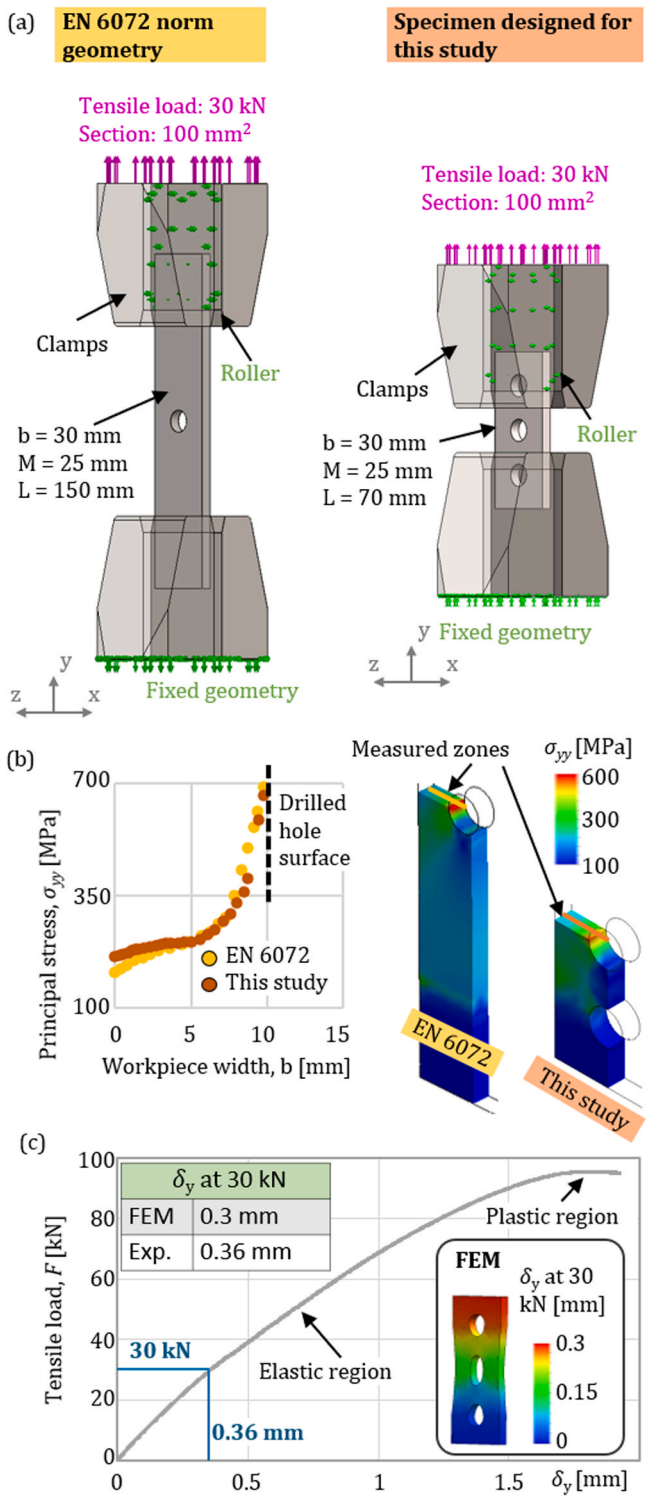

Fig. 10. (a) FEM models, boundary conditions and loads for fatigue specimen validation; (b) Stress distribution along the width of the specimen at the central hole; (c) Experimental validation of the FEM models using a uniaxial tensile test.

Cooling and lubrication had a greater influence on the fatigue strength of the specimens than the tool wear, increasing it by 48 % on average when drilling with LCO_2+MQL compared to dry. This increase in fatigue life could be linked to an improved surface roughness and a smaller burr (which was the zone of crack nucleation) when using LCO_2+MQL assistance in comparison to dry drilling (Fig. 9). The results agree with the studies [32,33], which link surface topography to fatigue life.

3.2.3. *Durability of selected functional unit*

As mentioned in the methodology, to simplify the study, the durability of the drilled CFRP stringer to Ti6Al4V stringer fitting assemblies of the Boeing 787 Dreamliner were assessed with FEM simulations, using the experimental fatigue strength data of the drilled CFRP/Ti6Al4V stacks.

For this study, the assembly of a single stringer to stringer fitting was modelled and simulated with SolidWorks Simulation software. High order quadratic elements were employed with a size that allowed to observe the stress distribution across the thickness of the stringer fitting and around the assembly holes. To reduce the computational cost, a geometric simplification of the model was made by adding a symmetry plane (Fig. 12a). A simple bending case was modelled as the purpose of the Ti6Al4V stringer fittings is to reduce the compressive stresses on the CFRP when the wing bends upwards. The area with the fixed boundary condition represents the assembly point between the stringers of the wing and the wing-box, therefore the movement and bending moments in all axes have been fully constrained. Two bolted joints were added to assemble the CFRP stringer to the Ti6Al4V stringer fitting (Fig. 12a).

The static bending stress case showed that the critical section of the assembly is located at the rear holes of the Ti6Al4V stringer fitting (Fig. 12b). To define the magnitude of the upward force on the CFRP stringer, a sensitivity analysis was carried out varying the load until the maximum stress at the critical point reached approximately 50 % of the Ti6Al4V yield strength. As shown in Fig. 12b, a load of 2500 N applied to the CFRP stringer produced a maximum stress of 481 MPa at the rear holes of the Ti6Al4V stringer fitting, corresponding roughly to 50 % of its yield strength. This load magnitude ensured that the stresses appearing in the FEM simulations fitted the values in the S-N curves obtained experimentally via fatigue testing specimens. The boundary conditions represent the dominant in-service loading path during wing bending, while secondary effects such as torsion, or thermal loads (negligible for hole-edge stresses) were disregarded.

Knowing the stress strain field, the fatigue strength of the assembly was calculated using the SolidWorks Simulation fatigue module. The S-N curves experimentally obtained for the CFRP and Ti6Al4V materials drilled in dry and with assistance of LCO_2+MQL were added to the material properties of the SolidWorks Simulation fatigue module. In order to reduce the uncertainties created by tool wear, and assuming that in aeronautical applications the tools are replaced before reaching the end of life, the fatigue strength curves obtained for the fresh tools were employed. The fatigue life of the component was determined by the most critical section, this is, the zone with the greatest stresses (Fig. 12b). The improvement in the fatigue strength of the Ti6Al4V phase of the stack when drilled with LCO_2+MQL resulted in a 52 % improvement in the expected fatigue life of the assembly (Fig. 12c).

3.3. *Life cycle assessment*

The LCA to compare the impact that different coolants have on the sustainability of machining processes, considering their influence on tool life and part durability, was carried out under certain assumptions and with defined boundary conditions. The monitored input and output flows to manufacture the functional unit were inserted in a life cycle inventory (LCI), and environmental impacts were associated to them using environmental databases to complete the life cycle impact assessment (LCIA).

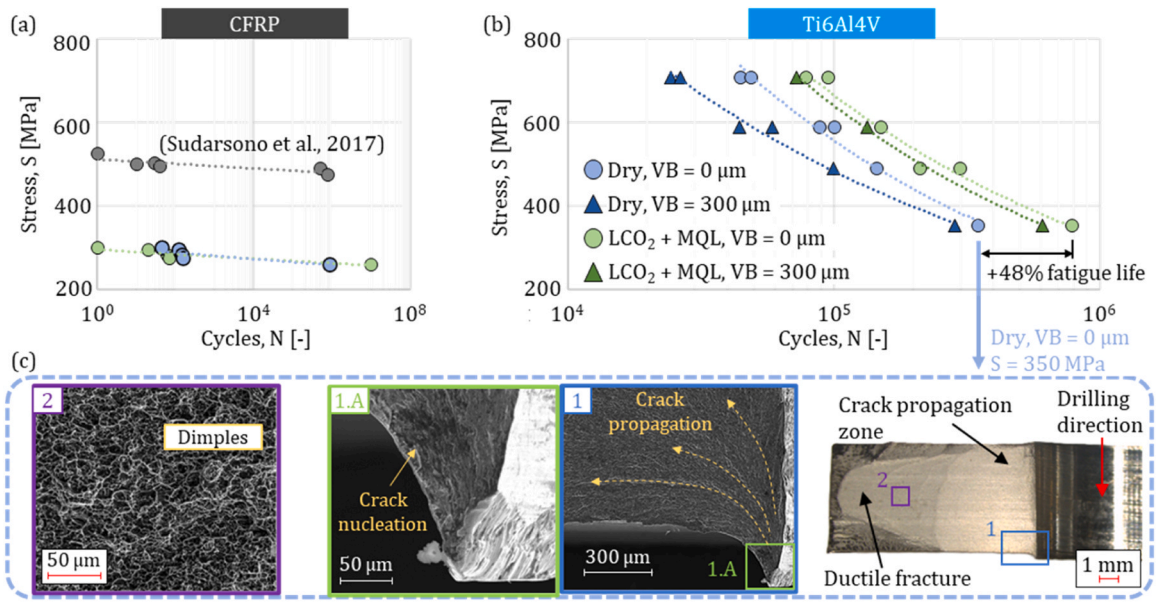

Fig. 11. S-N curves achieved for specimens drilled in dry and LCO_2+MQL assisted conditions at different tool wear levels: (a) CFRP; (b) Ti6Al4V, (c) Crack initiation at Ti6Al4V machined surfaces, crack propagation and ductile fracture zones.

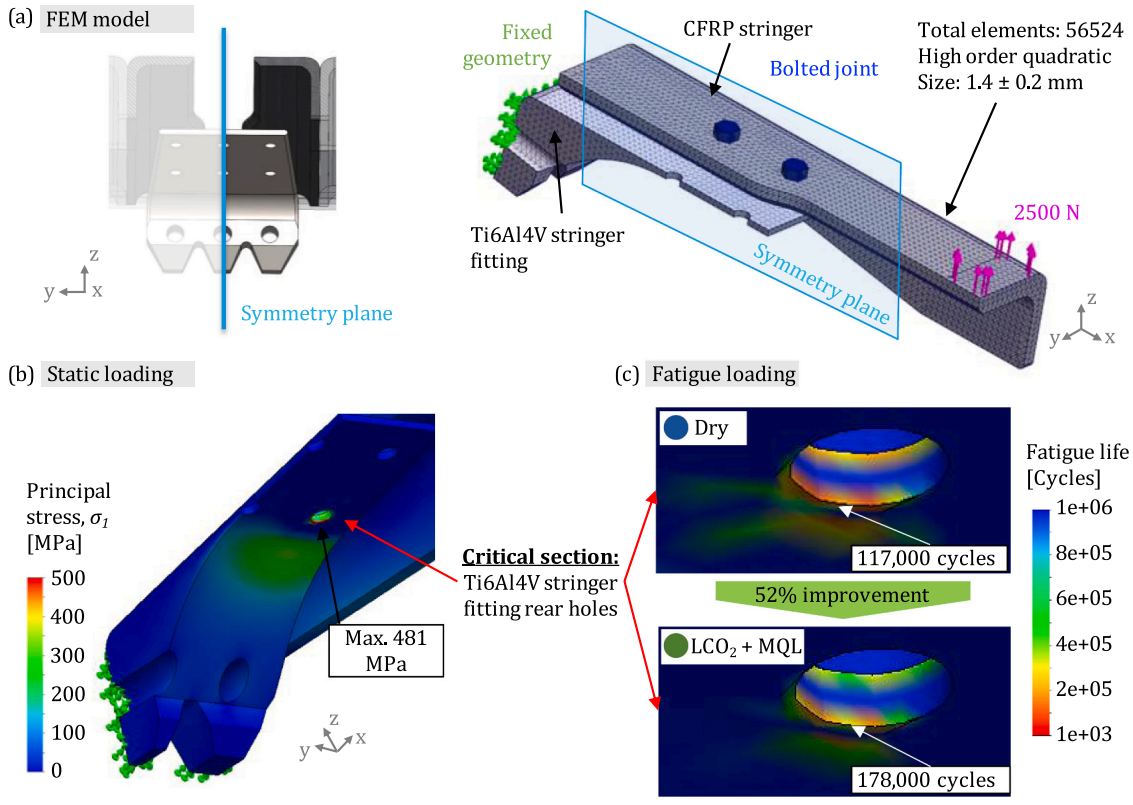

Fig. 12. (a) Symmetry simplification, boundary conditions and leads applied to the FEM model; (b) Principal stress results from the static flexural case simulation, (c) Estimated fatigue life of the critical section.

3.3.1. Functional unit, goal, scope and assumptions for the life cycle inventory (LCI)

The functional unit selected for this study was the fabrication and repair of the CFRP stringer to Ti6Al4V stringer fitting assembly in Boeing 787 Dreamliner aircrafts, as already mentioned in the case study description (Fig. 3). The goal of the LCA performed is to estimate the environmental impact of dry drilling these assemblies made out of CFRP/Ti6Al4V stacks and compare it to that of LCO_2+MQL assisted drilling. The analysis considers all phases of the aircraft life cycle and the scope of the study is thereby cradle-to-cradle. Of the various input and output flows in machining operations, only those measured empirically were considered, being a comparative case study between two cooling/lubrication scenarios. Fig. 13 summarizes the flows considered within the boundaries the LCA. The consumption of energy, coolant and tools,

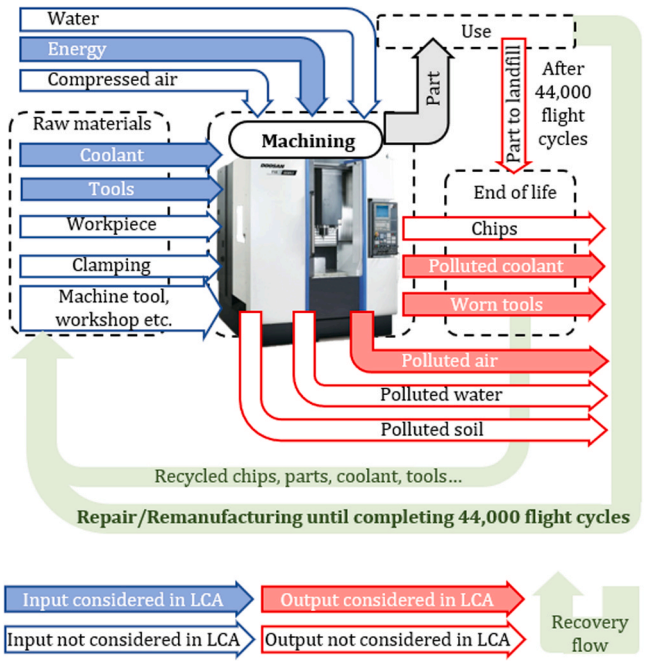

Fig. 13. Material and energy input and output flows associated with the machine tool considered in the LCA.

as well as the emission of PM2.5 particles were measured during the drilling experiments.

Several assumptions were made regarding the fatigue strength of the functional unit, approximated with FEM simulations and empirical data, to estimate its influence on the environmental footprint of the machining process. It was assumed that the critical load modelled in Fig. 12a occurs on average 10 times during a flight cycle of the aircraft. A preliminary sensitivity analysis (5 and 20 events per flight) confirmed that this assumption affects the absolute repair interval but not the relative difference between the dry and LCO_2+MQL scenarios. In all cases, the improved fatigue performance of the Ti6Al4V holes drilled with LCO_2+MQL led to a 52 % lower number of required repairs, and therefore the same proportional reduction in drilled holes.

Based on this proportional scaling, a value of 10 critical loads per flight cycle was adopted because it yields a repair interval for the LCO_2+MQL case (~17,800 cycles) that is consistent with the 18,000 cycle compliance threshold in the Boeing Service Bulletin B787–81205-SB570018–00 (Section 5, Compliance) [38]. This ensured realistic in-service conditions in one of the experimental cases. For the dry drilling case, with the predicted fatigue life (Fig. 12c), the aircraft would need to be repaired every 11,700 flight cycles. Additionally, it is assumed that a repaired hole will have the same in-service life as a new one. This follows the original manufacturer's statement that accomplishment of the bulletin's modification prevents an unacceptable reduction of the fatigue; accordingly, compliant repairs are treated as restoring baseline durability. If repaired holes were to exhibit a shorter life, the repair interval would scale proportionally for both scenarios and the relative environmental comparison would remain unchanged.

Due to the low oil consumption of MQL, this lubrication technique is often considered as near-dry machining [12,26]. Therefore, for modelling the LCA it was assumed that all MQL oil consumed is either evaporated or released as airborne emissions, thus no oil is recirculated. Power consumption was monitored using the internal signals of the machine-tool, and the average power consumption per hole across the entire life of the tool for dry and LCO_2+MQL assisted drilling of CFRP/Ti6Al4V stacks was calculated. This was then extrapolated to calculate the power consumption to drill all holes considering the holes per part and the number of repairs per lifetime of the plane. Some experimental inputs (e.g., clamping system, machine tool) were excluded from the LCA scope because their relative impact on the machining process is negligible due to their long service life and because they are unaffected by the cooling/lubrication conditions. Additionally, other flows, (e.g., compressed air, workpiece input, and chip outflow) were also excluded, as they remain constant across both cooling/lubrication scenarios. As described in the Boeing repair manual [38], the reparation operations involve redrilling of the holes. Therefore, no additional workpiece material input is needed nor scrap output is generated by the repairs.

For the specific case of dry and LCO_2+MQL assisted drilling of CFRP/Ti6Al4V stacks, no water is used during the machining process itself. Similarly, as the MQL oils only produce airborne particle emissions, no water or soil is contaminated by the coolant. Therefore, being this a comparative LCA between two cooling/lubrication techniques, water consumption input flow, as well as polluted water outflows were not considered. The impact created by the transportation of LCO_2 bottles and MQL oil was considered.

Table 4
Life cycle inventory of the input and output flows for dry and LCO_2+MQL assisted drilling.

		DRY	LCO_2+MQL
Part durability	Expected flight cycles during service life	44,000	44,000
	Flight cycles before repair	11,700	17,800
	Number of required repairs per aircraft service life	3.76	2.47
	Holes per repair (assumption)	200	200
	Total drilled holes per aircraft service life	**752.14**	**494.38**
Tools (input)	Tool life [holes]	65	135
	Tools per aircraft service life	11.57	3.66
	Tungsten carbide mass per drill bit (g)	73	73
	Consumed tool material per aircraft service life [g]	**844.71**	**267.33**
Coolant (input)	LCO_2 flow rate [g/min]	0	100
	MQL flow rate [mL/h]	0	40
	MQL density [g/cm^3]	–	0.87
	LCO_2 per aircraft service life [g]	**0.00**	**2070.86**
	MQL per aircraft service life [g]	**0.00**	**12.01**
Power (input)			
a) Cutting power	Average cutting power of the spindle per hole [kWh]	0.0015	0.00098
	Average cutting power of the Z axis per hole [kWh]	0.00167	0.00197
	Cutting power consumption per aircraft service life [kWh]	2.38	1.46
b) Non-cutting power	Power demand in standby [kW]	0.80	0.80
	Standby time for tool-changing per plane service life [h]	1.16	0.37
	Standby time for coolant operation per plane service life [h]	0	0.11
	Standby time power per aircraft service life [kWh]	0.93	0.38
c)Auxiliary equipment	Power consumption by coolant equipment [kWh]	0	0.10
	Total power consumption per aircraft service life [kWh]	**3.31**	**1.94**
Scrap (output)	CFRP chips [cm^3/hole]	0.39	0.39
	Ti6Al4V chips [cm^3/hole]	0.39	0.39
	Scrap CFRP mass per aircraft service life [g]	**502**	**330**
	Scrap Ti6Al4V mass per aircraft service life [g]	**1308**	**860**
Polluted air (output)	Average PM 2.5 per 30 holes operation [mg/m^3]	0.25	18.00
	Sampled volume [m^3]	6.75	6.75
	PM 2.5 emissions per aircraft service life [g]	**0.04**	**2.00**

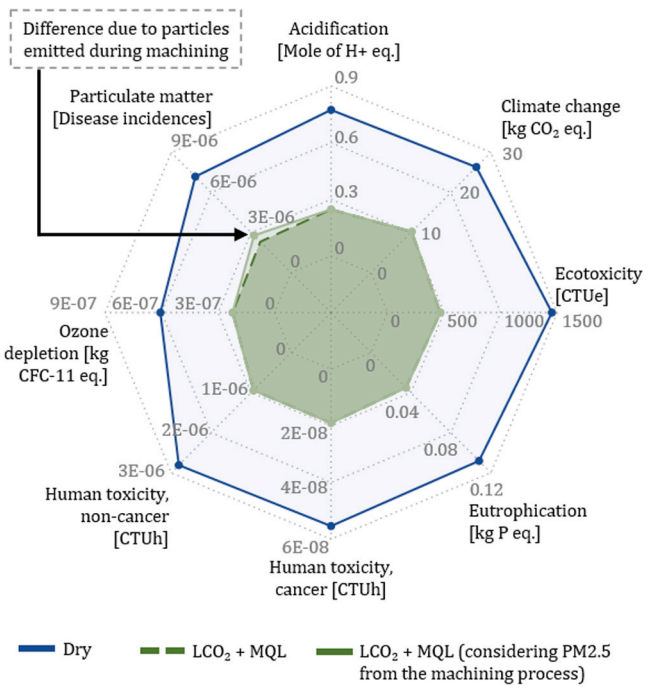

Fig. 14. Comparison of the total values of different impact factors for dry and LCO_2+MQL assisted drilling cases.

3.3.2. Life cycle inventory (LCI)

All experimentally measured resource and energy inputs, together with the airborne pollution outflows, were scaled to the functional unit: the fabrication and repairs of the CFRP stringer to Ti6Al4V stringer fitting assembly in Boeing 787 Dreamliner aircrafts, for their expected service life. The most relevant experimental and normalized data are summarized in the LCI in Table 4.

The conversion from experimental per-hole or time-dependent data to aircraft-level units was performed through a multi-step aggregation procedure. First, fatigue-life simulations estimated that assemblies drilled in dry conditions would require repair after 11,700 flight cycles, whereas those drilled with LCO_2+MQL could endure 17,800 cycles. Using Boeing's expected aircraft service life of 44,000 flight cycles [38], the number of required repairs per aircraft was calculated. Assuming 200 holes per repair, the total number of drilled holes over the aircraft lifetime was calculated for each scenario. Considering that tools are discarded after reaching 0.3 mm of flank wear (as specified in ISO 3685), the corresponding number of cutting tools required for the aircraft repairs was then estimated. It was also assumed that all machined material is converted to scrap.

Each measured experimental input or output (tool life, energy demand, coolant consumption, scrap mass, PM2.5 emissions) was then scaled by the total number of holes and converted to consistent units (e.g., amount of tools to tungsten carbide mass, kWh to MJ, g/min to g, etc.), to produce the life-cycle inventory aligned with the functional unit. To calculate energy consumption from measured power, experimentally determined cycle-time data were used: the tool-change duration was 6 min, and the cutting time for drilling a 10 mm CFRP/Ti6Al4V stack with the selected parameters was 2.5 s. Standby times required to extract coolant particles and safely open the machine-tool were 0 s for dry drilling and 75 s for LCO_2+MQL, as reported in [43].

3.3.3. Life cycle impact assessment (LCIA)

The system was modeled in the software LCA for experts (formerly GaBi), employing the generic database ecoinvent 3.9.1. The life cycle impact assessment methodology used was the Environmental footprint 3.1. (EF3.1.) [49].

The EF3.1. method includes several impact categories, however just 8 of them were selected for this study based on other LCA studies from the literature [12]. Namely, water acidification, climate change potential, ecotoxicity, eutrophication, human toxicity (cancer and non-cancer), ozone depletion and particulate matter. All these impact categories are presented in standardized units, that consider the contribution of the input and output flows of the LCI using equivalences defined in the LCIA methodology.

3.3.4. LCA results and interpretation

The LCA results given by the software show a great reduction of all considered impact categories when drilling the CFRP/Ti6Al4V components with LCO_2+MQL assistance (Fig. 14). On average a reduction of 60–70 % is achieved in all impact categories when using LCO_2+MQL assisted drilling. This is mainly due to the fact that the drilled components have better durability, reducing the need for component repair and the use of more resources compared to dry drilling.

The PM2.5 airborne particles measured on the workshop floor had a clear effect on the impact category of particulate matter. This shows that the oil mist cloud generated by the LCO_2+MQL cooling and lubrication can be of relevance in the overall environmental footprint of the machined component, although it affects a very localized area like the machine shop floor air. In the EF 3.1 methodology, the "Particulate matter: Disease Incidences" impact factor is calculated from weighted emission factors for processes such as energy generation, tool manufacturing, and material processing. In this study, we complemented these database-based emissions with experimentally measured airborne particles from the machining process itself. Including the measured values in the EF 3.1 LCI increased the particulate matter impact factor by about 20 % for the LCO_2+MQL condition, showing that adding empirical workshop-emission data improves the completeness and accuracy of LCA results. The finding underscores the relevance of clean air environments in our work areas [2].

Fig. 15 shows a detailed breakdown of the contribution of the individual consumption flows to the different impact categories. The outflow of particle emissions was included in the coolant consumption, since the particles are mainly generated by the coolant. As can be seen, the most relevant consumption flow is the cutting tool. This is due to the extraction and processing of tungsten carbide being an energy intensive process [13]. The environmental impact of the coolant comes due to the liquefaction of the carbon dioxide, the synthesis of oils for lubrication, and the airborne pollution generated by the use of such coolants in the workshop. Since LCO_2+MQL doubled the tool life in comparison to dry drilling, the environmental impact linked to tool production is considerably lower.

The improved environmental performance of LCO_2+MQL assisted drilling compared to dry drilling demonstrates that the use of additional resources like the coolant can be environmentally favorable in cases where tool life and part durability are improved. This observation contrasts with other studies conducting LCA studies that adopt a gate-to-gate scope, without considering the influence of the machining process on the performance of the manufactured components [26].

The proposed framework effectively integrates machining-induced surface quality into environmental assessments through part-durability evaluation. It is broadly applicable to other finish machining operations that define the final surface integrity of a component and thus influence its fatigue performance. The method is particularly relevant for components whose service life is governed by surface finish (e.g., metallic parts where critical features are machined). In contrast, cases dominated by internal defects or non-machined geometries may show weaker correlations. This scalability highlights the framework's potential to extend durability awareness into sustainability analyses and cradle-to-cradle LCAs across diverse machining processes.

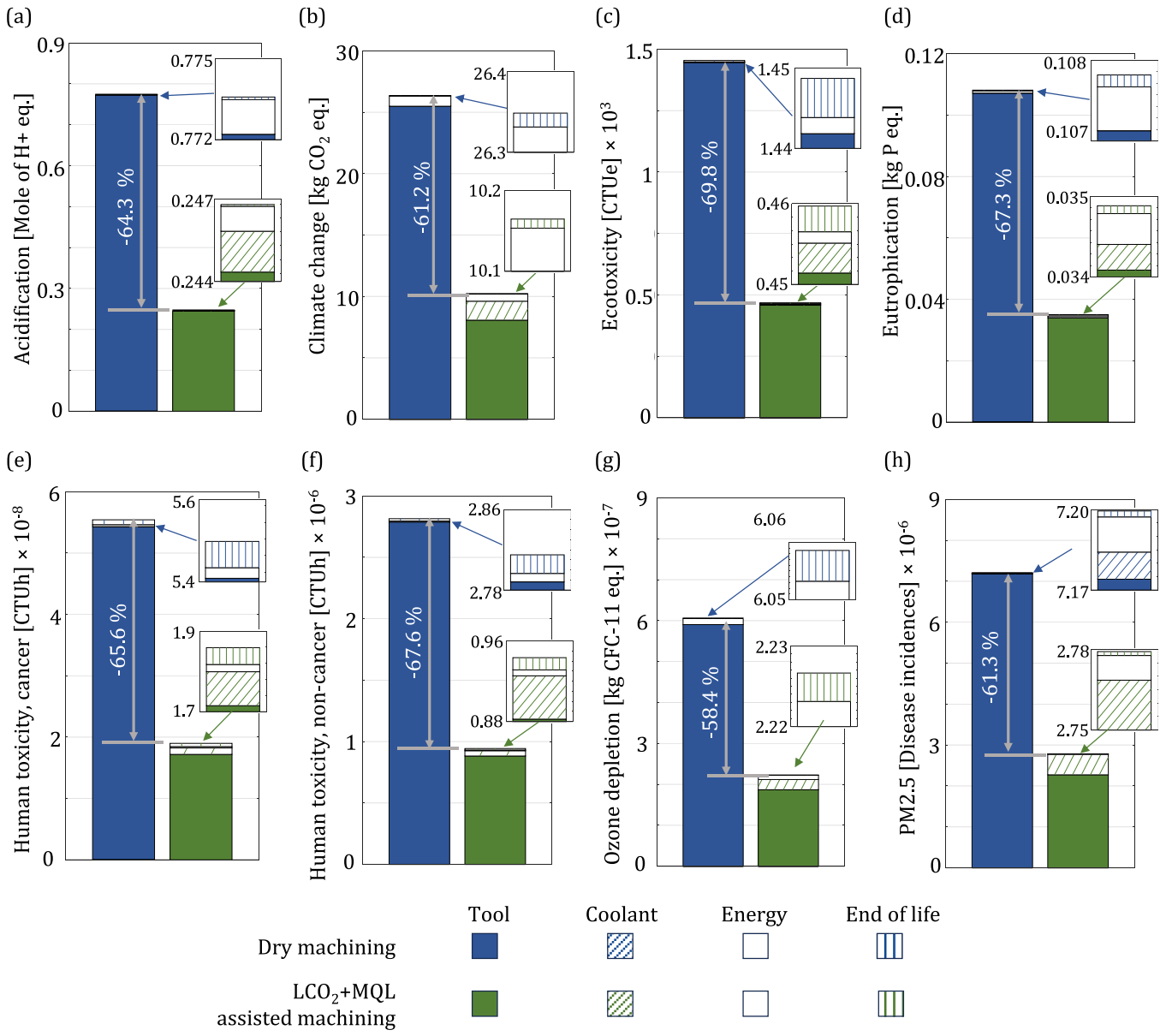

Fig. 15. Contribution to different impact categories for dry and LCO_2+MQL assisted drilling: (a) Acidification; (b) Climate change; (c) Ecotoxicity; (d) Eutrophication; (e) Human toxicity, cancer; (f) Human toxicity, non-cancer; (g) Ozone depletion, (h) Particulate matter, PM2.5.

4. Conclusions

In this paper a cradle-to-cradle LCA is carried out, and a new method is proposed to consider the influence of the quality of machined parts on the environmental impact. Machining tests and fatigue characterization of drilled components were performed to complete the life cycle inventory of the functional unit in an aeronautical case study. The main findings are as follows:

- The novel framework links machining-induced surface integrity to part durability within a cradle-to-cradle LCA. It is broadly applicable to finishing operations where machined surface quality governs fatigue performance. Its scalability may be more limited in cases where durability is dominated by internal material defects or non-machined geometries.
- The cutting tool was identified as the dominant contributor to the total environmental impact for the selected aeronautical LCA case study, exceeding the effects of energy and coolant use. Using LCO_2+MQL cooling and lubrication improved tool life by 225 % compared to dry drilling, resulting in a 60–70 % reduction in all environmental impact categories.
- Including part durability in the LCA influenced the overall material and energy flows required by the machining process. Despite LCO_2+MQL having a greater coolant consumption compared to dry drilling, it resulted in a more sustainable scenario for drilling CFRP/Ti6Al4V stack components. This was due to the combination of longer tool life and improved part durability, resulting in less resource and energy requirements for the repairs over the useful life of the Boeing 787 Dreamliner aircraft, and thus in a 70 % reduction in the environmental impact.
- The quality of the holes had little effect on the fatigue strength of drilled CFRP components due to the defects present in the material (voids, fiber discontinuities, etc.). Regarding Ti6Al4V phase of the stack, a 48 % improvement was obtained on average for the holes drilled with LCO_2+MQL assistance, regardless of the wear of the tool. Combining empirical fatigue strength data with FEM simulations of the functional unit, showed that stringer to stringer fitting assembly

between the aircraft fuselage and wing drilled with LCO_2+MQL were 52 % more durable than the ones drilled in dry.
- Empirical measurement of airborne particles emitted in the workshop had a relevant impact on the equivalent disease incidences due to particulate matter (PM2.5). This shows the importance that local emissions can have on the total environmental impact of machining.

CRediT authorship contribution statement

I. Rodriguez: Conceptualization, Data curation, Formal analysis, Investigation, Methodology, Visualization, Writing – original draft. **P.J. Arrazola:** Conceptualization, Funding acquisition, Project administration, Resources, Supervision, Writing – review & editing. **M. Mori:** Methodology, Data curation Formal analysis, Writing – review & editing. **G. Ortiz-de-Zarate:** Methodology, Formal analysis, Visualization, Writing – review & editing. **A. Madariaga:** Methodology, Formal analysis, Validation, Writing – review & editing. **M. Cuesta:** Supervision, Validation, Writing – review & editing. **F. Pušavec:** Project administration, Resources, Supervision, Writing – review & editing.

Declaration of Competing Interest

The authors declare that they have no known competing financial interests or personal relationships that could have appeared to influence the work reported in this paper.

Acknowledgements

The authors would like to express their great appreciation to SECO Tools for providing the tools necessary to carry out this research work, as well as to the nG24 (KK-2024/0001) and TAILORSURF projects (PID2022–139655OB-I00) for their financial support.

References

[1] Precedence Research, Precedence-Research, 2024, Machining Market, Report Number: 2997.
[2] Shokrani A, Arrazola PJ, Biermann D, Mativenga P, Jawahir IS. Sustainable machining: recent technological advances. CIRP Ann Jan. 2024;73(2):483–508. https://doi.org/10.1016/j.cirp.2024.06.001.
[3] Jack Barrie, Ilmi Salminen, Patrick Schroder, and Jerome Stucki, National circular economy roadmaps: a global stocktake for 2024, Vienna, May 2024.
[4] Kara S, Hauschild M, Sutherland J, McAloone T. Closed-loop systems to circular economy: a pathway to environmental sustainability? CIRP Ann Jan. 2022;71(2):505–28. https://doi.org/10.1016/j.cirp.2022.05.008.
[5] Hauschild MZ, Rosenbaum RK, Olsen SI. Theory and practice. Life Cycle Assess 2018. https://doi.org/10.1007/978-3-319-56475-3_29.
[6] Salem A, Hegab H, Kishawy HA. An integrated approach for sustainable machining processes: assessment, performance analysis, and optimization. Sustain Prod Consum Jan. 2021;25:450–70. https://doi.org/10.1016/j.spc.2020.11.021.
[7] Rizzo A, et al. The critical raw materials in cutting tools for machining applications: a review. MDPI Ag 2020. https://doi.org/10.3390/ma13061377.
[8] Sivarupan T, Bermingham M, Ng CH, Sun S, Dargusch M. A review of the use of cryogenic coolant during machining titanium alloys. Sustain Mater Technol Jul. 2024;40. https://doi.org/10.1016/j.susmat.2024.e00946.
[9] Sarıkaya M, et al. Performance and wear analysis in machining of Co-based Haynes 25/L605 superalloy using sustainable cooling/lubrication agencies. Sustain Mater Technol Apr. 2025;43. https://doi.org/10.1016/j.susmat.2025.e01268.
[10] Alswat HM, Mativenga PT. Modelling the direct and embodied energy requirements of machining. J Clean Prod Sep. 2022;366. https://doi.org/10.1016/j.jclepro.2022.132767.
[11] Quintana G, Ciurana J. Chatter in machining processes: A review. May 2011. https://doi.org/10.1016/j.ijmachtools.2011.01.001.
[12] Pereira O, Rodriguez A, Fernández-Abia AI, Barreiro J, López de Lacalle LN. Cryogenic and minimum quantity lubrication for an eco-efficiency turning of AISI 304. J Clean Prod 2016;139:440–9. https://doi.org/10.1016/j.jclepro.2016.08.030.
[13] Furberg A, Arvidsson R, Molander S. Environmental life cycle assessment of cemented carbide (WC-Co) production. J Clean Prod Feb. 2019;209:1126–38. https://doi.org/10.1016/j.jclepro.2018.10.272.
[14] Kokare S, Oliveira JP, Godina R. Life cycle assessment of additive manufacturing processes: A review. J Manuf Syst Jun. 2023;68:536–59. https://doi.org/10.1016/j.jmsy.2023.05.007.
[15] Favi C, Murgese L, Villazzi N, Gallozzi S, Mandolini M, Marconi M. Integrating life cycle engineering into design for additive manufacturing: a review. J Manuf Syst Oct. 2025;82:599–631. https://doi.org/10.1016/j.jmsy.2025.07.010.
[16] Pusavec F, Krajnik P, Kopac J. Transitioning to sustainable production - part I: application on machining technologies. J Clean Prod Jan. 2010;18(2):174–84. https://doi.org/10.1016/j.jclepro.2009.08.010.
[17] Mia M, et al. Multi-objective optimization and life cycle assessment of eco-friendly cryogenic N2 assisted turning of Ti-6Al-4V. J Clean Prod Feb. 2019;210:121–33. https://doi.org/10.1016/j.jclepro.2018.10.334.
[18] Pereira O, Urbikaín G, Rodríguez A, Calleja A, Ayesta I, López de Lacalle LN. Process performance and life cycle assessment of friction drilling on dual-phase steel. J Clean Prod 2019;213:1147–56. https://doi.org/10.1016/j.jclepro.2018.12.250.
[19] Priarone PC, Robiglio M, Settineri L. On the concurrent optimization of environmental and economic targets for machining. J Clean Prod Jul. 2018;190:630–44. https://doi.org/10.1016/j.jclepro.2018.04.163.
[20] Filleti RAP, Silva DAL, da Silva EJ, Ometto AR. Productive and environmental performance indicators analysis by a combined LCA hybrid model and real-time manufacturing process monitoring: a grinding unit process application. J Clean Prod Sep. 2017;161:510–23. https://doi.org/10.1016/j.jclepro.2017.05.158.
[21] Agrawal C, Wadhwa J, Pitroda A, Pruncu CI, Sarikaya M, Khanna N. Comprehensive analysis of tool wear, tool life, surface roughness, costing and carbon emissions in turning Ti–6Al–4V titanium alloy: cryogenic versus wet machining. Tribol Int Jan. 2021;153. https://doi.org/10.1016/j.triboint.2020.106597.
[22] Khanna N, Shah P, Wadhwa J, Pitroda A, Schoop J, Pusavec F. Energy consumption and lifecycle assessment comparison of cutting fluids for drilling titanium alloy. Procedia CIRP. Elsevier B.V.; 2021. p. 175–80. https://doi.org/10.1016/j.procir.2021.01.026.
[23] Faga MG, Priarone PC, Robiglio M, Settineri L, Tebaldo V. Technological and sustainability implications of dry, near-dry, and wet turning of Ti-6Al-4V alloy. Int J Precis Eng Manuf Green Technol Apr. 2017;4(2):129–39. https://doi.org/10.1007/s40684-017-0016-z.
[24] Liu ZY, Li C, Fang XY, Guo YB. Cumulative energy demand and environmental impact in sustainable machining of inconel superalloy. J Clean Prod Apr. 2018;181:329–36. https://doi.org/10.1016/j.jclepro.2018.01.251.
[25] Jamil M, et al. Sustainable milling of Ti–6Al–4V: A trade-off between energy efficiency, carbon emissions and machining characteristics under MQL and cryogenic environment. J Clean Prod Jan. 2021;281. https://doi.org/10.1016/j.jclepro.2020.125374.
[26] Khanna N, Prajapati R, Bolar G. Fabrication, machining (dry vs. cryogenic) and life cycle analysis of hybrid titanium composite laminates (HTCL). Mach Sci Technol 2024. https://doi.org/10.1080/10910344.2024.2369856.
[27] Khanna N, Shah P, de Lacalle LNL, Rodríguez A, Pereira O. In pursuit of sustainable cutting fluid strategy for machining Ti-6Al-4V using life cycle analysis. Sustain Mater Technol Sep. 2021;29. https://doi.org/10.1016/j.susmat.2021.e00301.
[28] Khanna N, Airao J, Kshitij G, Nirala CK, Hegab H. Sustainability analysis of new hybrid cooling/lubrication strategies during machining Ti6Al4V and Inconel 718 alloys. Sustain Mater Technol Jul. 2023;36. https://doi.org/10.1016/j.susmat.2023.e00606.
[29] Khanna N, et al. In pursuit of sustainability in machining thin walled α-titanium tubes: An industry supported study. Sustain Mater Technol Jul. 2023;36. https://doi.org/10.1016/j.susmat.2023.e00647.
[30] Korkmaz ME, Gupta MK, Çelik E, Ross NS, Günay M. A sustainable cooling/lubrication method focusing on energy consumption and other machining characteristics in high-speed turning of aluminum alloy. Sustain Mater Technol Jul. 2024;40. https://doi.org/10.1016/j.susmat.2024.e00919.
[31] He Y, Tian X, Li Y, Wang Y, Wang Y, Wang S. Modeling and analyses of energy consumption for machining features with flexible machining configurations. J Manuf Syst Jan. 2022;62:463–76. https://doi.org/10.1016/j.jmsy.2022.01.001.
[32] Arola D, Williams CL. Estimating the fatigue stress concentration factor of machined surfaces. Int J Fatigue 2002;24(September):923–30. https://doi.org/10.1016/S0142-1123(02)00012-9.
[33] Novovic D, Dewes RC, Aspinwall DK, Voice W, Bowen P. The effect of machined topography and integrity on fatigue life. Int J Mach Tools Manuf 2004;44(2–3):125–34. https://doi.org/10.1016/j.ijmachtools.2003.10.018.
[34] Xu J, Mkaddem A, El Mansori M. Recent advances in drilling hybrid FRP/Ti composite: a state-of-the-art review. Compos Struct 2016;135:316–38. https://doi.org/10.1016/j.compstruct.2015.09.028.
[35] M'Saoubi R, et al. High performance cutting of advanced aerospace alloys and composite materials. CIRP Ann Manuf Technol 2015;64(2):557–80. https://doi.org/10.1016/j.cirp.2015.05.002.
[36] Turner J, Scaife RJ, El-Dessouky HM. Effect of machining coolant on integrity of CFRP composites. Adv Manuf Poly Compos Sci 2015;1(1):54–60. https://doi.org/10.1179/2055035914Y.0000000008.
[37] Dominic Gates, Boeing 787's wing fix passes crucial test, sources say, The Seattle Times, 2009. Accessed: Feb. 25, 2024. [Online]. Available: ⟨https://www.seattletimes.com/business/boeing-787s-wing-fix-passes-crucial-test-sources-say/⟩.
[38] Boeing. Alert Serv Bull B 2015;787.
[39] Rodriguez I, Arrazola PJ, Cuesta M, Pušavec F. Hole quality improvement in CFRP/Ti6Al4V stacks using optimised flow rates for LCO2 and MQL sustainable cooling/lubrication. Compos Struct Feb. 2024;329. https://doi.org/10.1016/j.compstruct.2023.117687.
[40] Davim JP, Rubio JC, Abrao AM. A novel approach based on digital image analysis to evaluate the delamination factor after drilling composite laminates. Compos Sci Technol 2007;67:1939–45. https://doi.org/10.1016/j.compscitech.2006.10.009.

[41] Duboust N, Watson M, Marshall M, O'Donnel GE, Kerrigan K. Towards intelligent CFRP composite machining: Surface analysis methods and statistical data analysis of machined fibre laminate surfaces. Proc Inst Mech Eng B J Eng Manuf 2021;235 (10):1602–17. https://doi.org/10.1177/0954405420960920.
[42] Cao S, et al. Investigation of CFRP damages induced by the interface high temperature and mixed tool wear mechanism in drilling of thin-walled CFRP / Ti stacks. Compos Struct 2023;323(ember 2022).
[43] Rodriguez I, Arrazola PJ, Pušavec F. The impact of airborne emissions from coolants and lubricants on machining costs. CIRP Ann Jan. 2024;73(1):77–80. https://doi.org/10.1016/j.cirp.2024.04.056.
[44] Xia T, Kaynak Y, Arvin C, Jawahir IS. Cryogenic cooling-induced process performance and surface integrity in drilling CFRP composite material. Int J Adv Manuf Technol 2016;82(1–4):605–16. https://doi.org/10.1007/s00170-015-7284-y.
[45] Lazoglu I, et al. Thermal analysis in Ti-6Al-4V drilling. CIRP Ann Manuf Technol 2017;66(1):105–8. https://doi.org/10.1016/j.cirp.2017.04.020.
[46] Sudarsono KO. Fatigue Behavior of Open-Holed CFRP Laminates with Initially Cut Fibers. Open J Compos Mater 2017;07(01):49–62. https://doi.org/10.4236/ojcm.2017.71003.
[47] Haeger A, Grudenik M, Hoffmann MJ, Knoblauch V. Effect of drilling-induced damage on the open hole flexural fatigue of carbon/epoxy composites. Compos Struct May 2019;215:238–48. https://doi.org/10.1016/j.compstruct.2019.02.025.
[48] Alam P, Mamalis D, Robert C, Floreani C, Ó Brádaigh CM. The fatigue of carbon fibre reinforced plastics - a review. Elsevier Ltd.; Jun. 01, 2019. https://doi.org/10.1016/j.compositesb.2019.02.016.
[49] European Comission, European Platform on LCA - EPLCA. Accessed: Nov. 10, 2024. [Online]. Available: ⟨https://eplca.jrc.ec.europa.eu/EnvironmentalFootprint.html⟩.